

ARTICLES

Excited-State Proton Transfer to Solvent from Phenol and Cyanophenols in Water

Shigeo Kaneko, Shigeyoshi Yotoriyama, Hitoshi Koda, and Seiji Tobita*

Department of Chemistry and Chemical Biology, Gunma University, Kiryu, Gunma 376-8515, Japan

Received: September 30, 2008; Revised Manuscript Received: December 27, 2008

The excited-state proton transfer (ESPT) to solvent from phenol (PhOH) and cyanophenols (CNOHs) in water was studied by means of time-resolved fluorescence and photoacoustic spectroscopy. A characteristic property of PhOH and CNOHs is that the fluorescence quantum yields of the deprotonated forms are remarkably small ($\leq 10^{-3}$) and the lifetimes are extremely short (≤ 30 ps). Time-resolved fluorescence measurements for PhOH, CNOHs, and their methoxy analogues at 298 K indicate that *o*- and *m*-cyanophenols (*o*- and *m*-CNOH) undergo rapid ESPT to the solvent water with rate constants of 6.6×10^{10} and $2.6 \times 10^{10} \text{ s}^{-1}$, respectively, whereas the fluorescence properties of PhOH and *p*-CNOH does not exhibit clear evidence of the ESPT reaction. Photoacoustic measurements show that photoexcitation of *o*- and *m*-CNOH in water results in negative volume changes, supporting the occurrence of ESPT to produce a geminate ion pair. In contrast, the volume contractions for the PhOH and *p*-CNOH solutions are negligibly small, which indicates that, in these compounds, the yields of solvent-separated ion pairs resulting from the ESPT are very small. The volume change per absorbed Einstein (ΔV_r) for *o*-CNOH is obtained to be $-5.0 \text{ mL Einstein}^{-1}$, which is much smaller than the estimated volume contraction per photoconverted mole (ΔV_R). This suggests that the geminate recombination between the ejected proton and the cyanophenolate anion occurs after rapid deactivation of the excited ion pair. In the temperature range between 275 and 323 K, the proton dissociation rates of *o*- and *m*-CNOH in H_2O and D_2O are slower than the solvent relaxation rates evaluated from the Debye dielectric relaxation time, indicating that the overall rate constant is determined mainly by the proton motion along the reaction coordinate.

Introduction

Since the original works of Förster¹ and Weller,² the excited-state proton transfer (ESPT) reactions of hydroxyaromatic molecules have been extensively investigated with particular interest on molecular mechanisms of proton transfer reactions in solution.^{3–11} Until recently, a number of experimental and theoretical studies were carried out for 1- and 2-naphthols as prototypes of hydroxyaromatic molecules. Their proton dissociation rate constants in water at 298 K were directly determined by time-resolved fluorescence measurements to be 2.5×10^{10} and $1.1 \times 10^8 \text{ s}^{-1}$, respectively.^{12,13} Robinson et al.^{12,14} have suggested that the basic rate of weak photoacids, such as 1- and 2-naphthols, is limited by rotational reorientation of water molecules, and therefore, weak acid dissociation in water cannot take place on time scales shorter than the Debye rotational correlation time. Huppert and collaborators^{15–18} have made comprehensive studies on the reversible proton dissociation and recombination of naphthol derivatives. Recently, Agmon has reported a very detailed description of ESPT reactions of naphthols on the basis of experimental and also theoretical studies.¹⁰

This wealth of information available on the ESPT reaction of naphthols in aqueous solution is contrasted by the absence of similar data on phenol (PhOH) and its derivatives. Wehry and Rogers¹⁹ investigated the influence of substituents upon the

ESPT equilibrium constant ($\text{p}K_a^*$) of a series of monosubstituted phenols. They found that the excited-state acidities can be correlated well with ground-state substituent constants evaluated by the Hammett and Taft equations and that conjugative effects are much more important, relative to inductive effects, in the excited states than in the ground state. Schulman et al.²⁰ investigated the prototropic dissociation and reprotonation in the S_1 state of *o*-, *m*-, and *p*-cyanophenols (CNOHs) by steady-state and time-resolved fluorescence measurements. They estimated the rate constants for the proton dissociation of *o*-, *m*-, and *p*-CNOH to be 4.0×10^8 , 1.9×10^8 and $2.8 \times 10^7 \text{ s}^{-1}$, respectively. Because the fluorescence decay times of CNOHs are in a picosecond time range, the time resolution (~ 1.7 ns) of their apparatus used for the lifetime measurements might not be sufficient to obtain the accurate proton dissociation rates. In spite of the recent development of ultrafast laser spectroscopy, there seems to be few reports on the ESPT dynamics of PhOH and CNOHs in aqueous solution. The extremely weak fluorescence intensity of the deprotonated anion of phenols seems to render direct measurement of ESPT difficult. This is in contrast with 1- and 2-naphthols that exhibit strong fluorescence from the deprotonated form.

Phenol is an important constituent of the chromophore (*p*-hydroxybenzylidene-imidazolidinone) of green fluorescent protein (GFP) which is now widely used as noninvasive, genetically encoded reporters in biochemistry and cell biology.^{21,22} It has been suggested that, in wild-type GFP (wtGFP), not only the

* Corresponding author. E-mail: tobita@chem-bio.gunma-u.ac.jp.

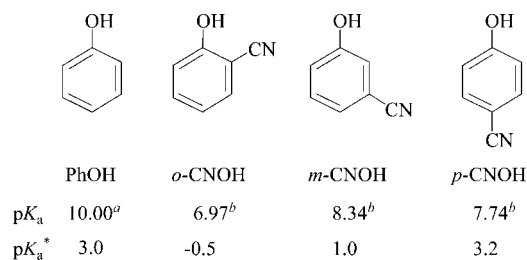


Figure 1. Structures and abbreviations of the sample compounds; pK_a values in the ground state and those in the S_1 state (pK_a^*) estimated by the Förster cycle method. ^aFrom ref 19. ^bFrom ref 20.

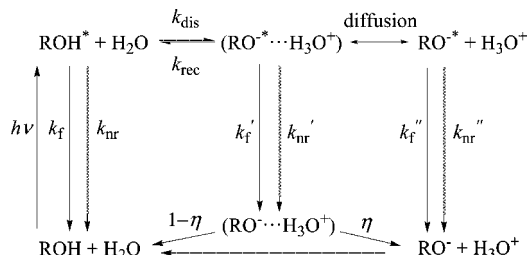


Figure 2. Kinetic scheme for prototropism of phenols in aqueous solution.

deprotonated form of the chromophore but also the protonated form, which exhibits an absorption peak at 398 nm, gives the characteristic green emission resulting from the ESPT reaction to water molecules in the vicinity of the chromophore in GFP.^{23–26} The tyrosine residue in proteins also possesses a phenol moiety as chromophore. The understanding of the ESPT reactions of phenol and its derivatives is, therefore, of great importance in biological studies as well as from fundamental aspects of proton transfer reactions.

In the present work, we investigated the ESPT to solvent of PhOH and CNOHs (see Figure 1) by time-resolved fluorescence and photoacoustic (PA) measurements. The ground-state pK_a values and those of the excited singlet (S_1) state (pK_a^*) are shown in Figure 1. The prototropic equilibrium of PhOH and CNOHs in the ground and S_1 states is depicted in Figure 2 along with the fluorescence and nonradiative deactivation processes from each excited species. This study was undertaken to answer the following questions: whether or not the ESPT to solvent occurs for PhOH and CNOHs in water, and, if it takes place, how fast are the rates and what factors determine the rate.

Experimental Section

Phenol (PhOH, Wako), *o*-cyanophenol (*o*-CNOH, Tokyo Kasei), *m*-cyanophenol (*m*-CNOH, JANSSEN CHEMICA), and *p*-cyanophenol (*p*-CNOH, Aldrich) were purified by vacuum sublimation. Their methoxy analogues, *o*-methoxybenzonitrile (*o*-CNOCH₃, Aldrich), *m*-methoxybenzonitrile (*m*-CNOCH₃, AVOCADO), and *p*-methoxybenzonitrile (*p*-CNOCH₃, Aldrich) were used without further purification, except for anisole (PhOCH₃, Wako) which was distilled under reduced pressure. Sodium dichromate (Na₂Cr₂O₇, Kanto) was used as received. Acetonitrile (Kanto) was purified by distillation. Cyclohexane (CH, Aldrich, spectrophotometric grade), ethanol (Kishida, spectroscopic grade), and methanol (Kishida, spectroscopic grade) were used as received. Deionized water was purified by using a Millipore (MILLI-Q-Labo). D₂O (Merck, > 99.8%) was used as received. H₂SO₄ (Wako, 97%, S. S. grade) or KOH (Kanto) was used to adjust the acid concentration of sample solutions.

Absorption and fluorescence spectra were recorded on an UV-vis spectrophotometer (Jasco, Ubest-50) and a spectrofluorometer (Hitachi, F-4010), respectively. Fluorescence quantum yields were determined by comparing the integrated intensities of the fluorescence spectra with that of standard quinine bisulfate in 0.5 M aqueous sulfuric acid solution ($\Phi_f = 0.546$)²⁷ or aniline in cyclohexane ($\Phi_f = 0.17$).²⁸

Nanosecond fluorescence lifetimes were measured with a time-correlated single-photon counting fluorimeter (Edinburgh Analytical Instrument, FL-900CDT). A nanosecond pulsed discharge lamp (pulse width, ~ 1.0 ns; repetition rate, 40 kHz) filled with hydrogen gas was used as the excitation light source. The solutions used in the nanosecond fluorescence lifetime measurements were degassed by freeze–pump–thaw cycles on a high vacuum line. Picosecond fluorescence lifetime measurements were made by using a femtosecond laser system which was based on a mode-locked Ti:sapphire laser (Spectra-Physics, Tsunami; center wavelength, 800 nm; pulse width, ~ 70 fs; repetition rate, 82 MHz) pumped by a CW green laser (Spectra-Physics, Millennia V; 532 nm, 4.5 W).²⁹ The repetition frequency was reduced to 4 MHz by using a pulse picker (Spectra-Physics, model 3980), and the third harmonic (266 nm; fwhm, ~ 250 fs) was used as the excitation source. The monitoring system consisted of a microchannel plate photomultiplier tube (MCP-PMT; Hamamatsu, R3809U-51) cooled to -20 °C and a single-photon counting module (Becker and Hickl, SPC-530). The fluorescence photon signal detected by the MCP-PMT and the photon signal of the second harmonic (400 nm) of the Ti:sapphire laser were used for the start and stop pulses of a time-to-amplitude converter in this system. The instrument response function had a half width of about 25 ps. The fluorescence time profiles were analyzed by deconvolution with the instrument response function.

PA measurements were made by using a Nd³⁺:YAG laser (Spectra Physics, GCR-130, pulse width 6 ns, 266 nm) as the excitation source.²⁹ The sample solution was irradiated by the laser beam after passing through a slit (0.5 mm width). The effective acoustic transit time was estimated to be ~ 340 ns. The laser fluence was varied by using a neutral density filter, and the laser pulse energy was measured with a pyroelectric energy meter (Laser Precision, RJP-753 and RJ7620). The PA signal detected by a piezoelectric detector (panametrics V103, 1 MHz) was amplified by using a wide-band high-input impedance amplifier (panametrics 5676, 50 kHz, 40 dB) and fed to a digitizing oscilloscope (Tektronix, TDS-744). The temperature of the sample solution was held to ± 0.02 °C.

Results and Discussion

Absorption and Fluorescence Properties of Phenol and Cyanophenols. Figure 3 shows the absorption and fluorescence spectra of PhOH, CNOHs (*o*-CNOH, *m*-CNOH, and *p*-CNOH), and their methoxy analogues (PhOCH₃; *o*-CNOCH₃, *m*-CNOCH₃, and *p*-CNOCH₃) at room temperature. The absorption spectra of PhOH and three CNOHs are little affected by the replacement of the hydroxyl group to the methoxy group. This shows that the electronic structures of PhOH and CNOHs are not altered significantly by the methoxy substitution. The fluorescence spectra of PhOH, *m*-CNOH, and *p*-CNOH almost coincide with those of their methoxy derivatives, except that the fluorescence spectra of the hydroxyl compounds are slightly red-shifted, probably because of hydrogen bonding interactions with solvent molecules.

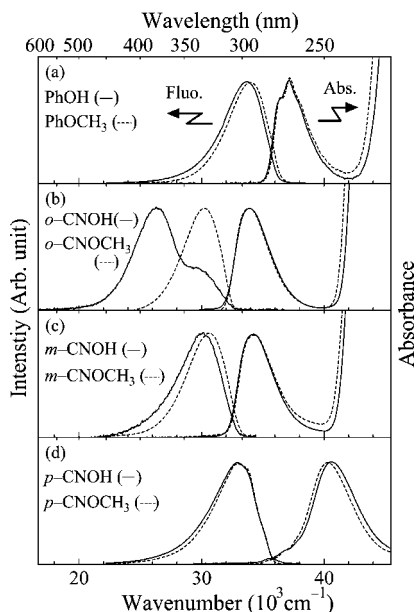


Figure 3. Absorption and fluorescence spectra of (a) PhOH ($\lambda_{\text{exc}} = 250$ nm) and PhOCH₃ ($\lambda_{\text{exc}} = 250$ nm), (b) *o*-CNOH (pH 4.0, $\lambda_{\text{exc}} = 235$ nm), and *o*-CNOCH₃ ($\lambda_{\text{exc}} = 260$ nm), (c) *m*-CNOH ($\lambda_{\text{exc}} = 240$ nm) and *m*-CNOCH₃ ($\lambda_{\text{exc}} = 260$ nm), (d) *p*-CNOH ($\lambda_{\text{exc}} = 250$ nm) and *p*-CNOCH₃ ($\lambda_{\text{exc}} = 250$ nm) in H₂O at room temperature. The pH adjustment of the sample solutions is not made except for *o*-CNOH (pH 4.0).

In contrast to the fluorescence spectra of PhOH, *m*-CNOH, and *p*-CNOH, *o*-CNOH exhibits dual fluorescence bands: normal and large Stokes-shifted fluorescence bands with maxima at 330 and 380 nm. The shorter-wavelength band resembles the fluorescence spectrum of the methoxy analogue. The excitation spectrum of the longer- and shorter-wavelength bands agreed with the absorption spectrum, indicating that both bands originate from the parent molecule. In the following discussions, it will be shown that the longer-wavelength band is due to the excited deprotonated form of *o*-CNOH which was produced by ESPT to solvent.

Figure 4 shows the absorption and fluorescence spectra of PhOH, CNOHs, and their deprotonated anions in aqueous solutions. The absorption and fluorescence spectra of the anions appear at much longer wavelengths compared with those of the protonated forms. It is noteworthy that the longer-wavelength band of *o*-CNOH is in fair agreement with the fluorescence spectrum of its anion. This also supports that in *o*-CNOH proton transfer to solvent takes place in the excited state.

As shown in Table 1, the fluorescence quantum yield (Φ_f) and lifetime (τ_f) of phenolate and cyanophenolate anions in water are extremely small, indicating that these excited anions undergo very rapid nonradiative deactivation from the S₁ state. This is in marked contrast to much larger Φ_f values of 1- and 2-naphtholate anions (0.12 and 0.57, respectively, in H₂O).³⁰ On the basis of on MO calculations, Wang et al.³¹ have reported that the almost nonfluorescent property of phenolate anion can be ascribed to the electronically forbidden nature of the S₁ ← S₀ transition of the phenolate anion which belongs to the C_{2v} point group. However, the extremely short fluorescence lifetimes of the phenolate anion and its cyano derivatives demonstrate that very rapid nonradiative processes are involved in these anions in water. The nonradiative process is attributable, at least partly, to photoinduced electron ejection, although the quantum yield for the electron ejection is reported to be less than 0.2, even for the phenolate anion.³² If the nonradiative deactivation

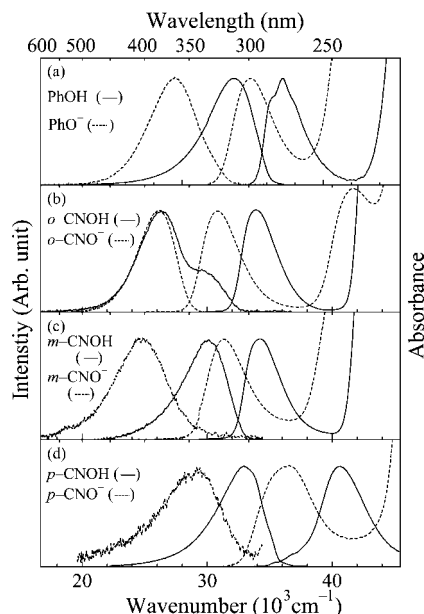


Figure 4. Absorption and fluorescence spectra of (a) PhOH ($\lambda_{\text{exc}} = 250$ nm) and PhO[−] ($\lambda_{\text{exc}} = 250$ nm), (b) *o*-CNOH (pH 4.0, $\lambda_{\text{exc}} = 235$ nm), and *o*-CNO[−] ($\lambda_{\text{exc}} = 250$ nm), (c) *m*-CNOH ($\lambda_{\text{exc}} = 240$ nm) and *m*-CNO[−] ($\lambda_{\text{exc}} = 240$ nm), (d) *p*-CNOH ($\lambda_{\text{exc}} = 250$ nm) and *p*-CNO[−] ($\lambda_{\text{exc}} = 260$ nm) in H₂O at room temperature. The pH adjustment of the sample solutions is not made except for *o*-CNOH (pH 4.0) and all the anions (pH 13).

TABLE 1: Fluorescence Quantum Yield (Φ_f) and Lifetime (τ_f) of Phenolate Anion and Cyanophenolate Anions in H₂O, D₂O, CH₃OH, and C₂H₅OH at 298 K

compound	Φ_f	τ_f (ps)			
		H ₂ O ^a	H ₂ O ^a	D ₂ O ^b	CH ₃ OH ^c
PhO [−]	8.0×10^{-4}	18	43	345	477
<i>o</i> -CNO [−]	1.0×10^{-3}	30	36	286	689
<i>m</i> -CNO [−]	2.5×10^{-4}	5	7	24	51
<i>p</i> -CNO [−]	5.3×10^{-4}	7	9	24	37

^a pH = 13. ^b pD = 13. ^c 1 M KOH.

is mainly due to the electron ejection from the fluorescent state, the cyano derivatives are expected to give longer lifetimes because of electron-withdrawing effects of the cyano group. The actual lifetimes show an opposite tendency (see Table 1). The deuterium isotope effects observed for the fluorescence lifetime and remarkable enhancement of the lifetimes in CH₃OH and C₂H₅OH suggest that the rapid deactivation processes of the cyanophenolate anion in water are associated with the hydrogen-bonding interactions between the phenolate oxygen atom (and/or the cyano group³³) and water molecules in addition to the electron ejection. We have found a similar remarkable water-induced quenching process for aniline and its derivatives.^{29,34}

The extremely weak fluorescence of the anions of PhOH and CNOHs makes it difficult to observe their ESPT process by steady-state fluorescence measurements (see Figure 3 and Table 1). Therefore, we carried out time-resolved fluorescence and PA measurements.

Proton Dissociation Rate of *o*-Cyanophenol in the S₁ State.

Photoprotolytic reactions of phenols in aqueous solution can be described by a two-step model as shown in Figure 2. In the first step, a rapid charge separation takes place and a solvent-stabilized ion pair is formed. This is followed by a diffusion step in which the hydrated proton is removed from the parent molecule. Agmon and collaborators¹⁰ have shown that this latter

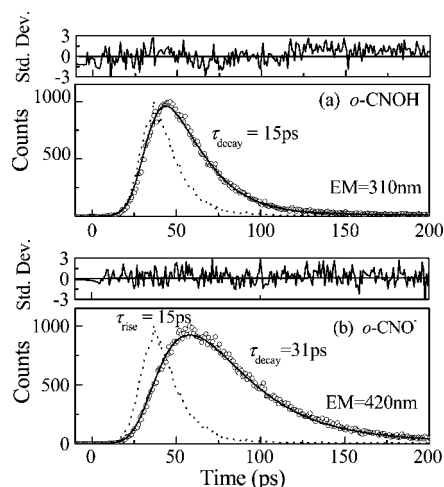


Figure 5. Fluorescence time profiles of *o*-CNOH in H₂O (pH 2.9) at 298 K monitored at (a) 310 nm and (b) 420 nm ($\lambda_{\text{exc}} = 266$ nm). The instrument response function is denoted by broken line. Standard deviation in panel a is worse than that in panel b because of very weak fluorescence intensity at 310 nm.

step is described by the Debye–Smoluchowski equation (DSE). In Figure 2, k_{dis} and k_{rec} denote the rate constants for adiabatic proton dissociation and reprotonation reactions, respectively. Because the decay rate of ${}^1\text{RO}^{-*}$ is very fast (see Table 1), the geminate-recombination as well as a diffusion second step can be neglected under moderately acidic conditions ($[\text{H}_3\text{O}^+] < 10^{-2}$ M).³⁵ Then, the fluorescence kinetics of ${}^1\text{ROH}^*$ and ${}^1\text{RO}^{-*}$ on excitation by a δ -pulse follows the monoexponential and biexponential laws, respectively,

$$I_{\text{f}}^{\text{ROH}}(t) = A_0 \exp\left(-\frac{t}{\tau}\right) \quad (1)$$

$$I_{\text{f}}^{\text{RO}^-}(t) = A_0' \left[\exp\left(-\frac{t}{\tau'}\right) - \exp\left(-\frac{t}{\tau}\right) \right] \quad (2)$$

where $1/\tau = k_{\text{f}} + k_{\text{nr}} + k_{\text{dis}} = 1/\tau_0 + k_{\text{dis}}$.

In order to determine the proton dissociation rate from ${}^1\text{ROH}^*$, the fluorescence time profile of *o*-CNOH in H₂O (pH 2.9) was taken by using the third harmonic (266 nm) of the mode-locked Ti:sapphire laser as the excitation source. In Figure 5, the fluorescence time profiles of the shorter-wavelength band (monitored at 310 nm) and the longer-wavelength band (monitored at 420 nm) of *o*-CNOH are shown along with the least-squares fitting curves based on eqs 1 and 2. The solid lines represent the deconvoluted best fit of (a) a single-exponential function and (b) a two-exponential function superimposed on the experimental data points, by using the parameters $\tau = 15$ ps and $\tau' = 31$ ps. It can be seen that both time profiles are well fitted by the kinetics described above; that is, the shorter-wavelength fluorescence band originates from the protonated form (*o*-CNOH), and the longer-wavelength fluorescence band is due to the deprotonated form (*o*-CNO[−]) produced by proton dissociation in the excited state. The decay time constant (31 ps) of the long-wavelength band is actually consistent with the lifetime (30 ps) of *o*-CNO[−] (see Table 1). The proton dissociation rate constant (k_{dis}) of *o*-CNOH in H₂O was determined to be $6.6 \times 10^{10} \text{ s}^{-1}$ from the proton dissociation time ($\tau = 15$ ps) by using the following equation,

$$k_{\text{dis}} = 1/\tau - 1/\tau_0 \quad (3)$$

where τ_0 was assumed to be equal to the lifetime (2.0 ns) of *o*-CNOCH₃ in H₂O (see Table 2). It is noted that the proton dissociation rate of *o*-CNOH in H₂O is faster than those of 1-naphthol ($2.5 \times 10^{10} \text{ s}^{-1}$) and 2-naphthol ($1.1 \times 10^8 \text{ s}^{-1}$).^{12,13}

Fluorescence Lifetime of Phenol and Cyanophenols and Their Methoxy Analogues. Although it has become apparent from the steady-state and time-resolved fluorescence measurements that *o*-CNOH in H₂O undergoes rapid proton transfer to solvent water in the S₁ state, it is still not clear whether the proton dissociation takes place similarly in the other compounds (PhOH, *m*-CNOH, and *p*-CNOH). If the proton dissociation process, which can compete with the other relaxation processes from the excited state (fluorescence, intersystem crossing, internal conversion, etc.) is involved also in these compounds, the fluorescence lifetimes should become much shorter than those of their methoxy analogues in which the proton cannot be split off. Hence, we measured the fluorescence lifetime of PhOH and CNOHs and their methoxy analogues in H₂O and in organic solvents, cyclohexane (CH) and acetonitrile. The fluorescence time profiles of these compounds followed single-exponential decay, and the fluorescence lifetimes were obtained as shown in Table 2. For the compounds with moderate acidity, it can be expected that the ESPT does not occur in organic solvents.⁹ Actually, the fluorescence lifetimes of PhOH and CNOHs in organic solvents are relatively long (2.0–7.0 ns) and are only slightly shorter than those of their methoxy analogues both in CH and CH₃CN. In contrast to the lifetimes in organic solvents, the fluorescence lifetimes of CNOHs in H₂O are remarkably short. In particular, the lifetime (0.015 ns) of *o*-CNOH is extremely short, which was ascribable to fast proton dissociation in the excited state. In the same manner, the short lifetime (0.037 ns) of *m*-CNOH in H₂O suggests the occurrence of the excited-state proton dissociation. The lifetime of *p*-CNOH in H₂O is one-order of magnitude longer than those of *o*- and *m*-CNOH in H₂O. Although the lifetime of *p*-CNOH in H₂O is much shorter than those in CH and CH₃CN, the methoxy analogue (*p*-CNOCH₃) also shows a similar tendency. It is therefore not clear whether proton dissociation occurs in *p*-CNOH or not.

Volume Changes Associated with ESPT of PhOH and CNOHs in Water. In order to examine the ESPT of PhOH and CNOHs in more detail, we made PA measurements.³⁶ The amplitude of PA signal H is attributable to the overall volume change arising from two contributions,

$$H = k(\Delta V_{\text{th}} + \Delta V_{\text{r}}) \quad (4)$$

where k is the instrumental constant, ΔV_{th} is the volume change of the solvent due to heat released by nonradiative deactivation process, and ΔV_{r} (ml Einstein^{−1}) is the structural volume change per absorbed Einstein, which includes any conformational variation due to photochemical processes and/or rearrangement of solvent. ΔV_{th} is related to the thermodynamic parameters as follows,

$$\Delta V_{\text{th}} = \alpha \left(\frac{\beta}{C_p \rho} \right) E_{\lambda} \quad (5)$$

where α is the fraction of absorbed energy released as heat within the effective acoustic transit time, β is the thermal

TABLE 2: Fluorescence Lifetimes of Phenol, Cyanophenols, and Their Methoxy Analogues in H₂O, CH₃, and CH₃CN at 298 K^a

compound	τ_f (ns)		
	H ₂ O	CH ₃	CH ₃ CN
PhOH	3.1	2.4	6.4
<i>o</i> -CNOH	0.015 ^b	3.6	2.1
<i>m</i> -CNOH	0.037	4.3	2.7
<i>p</i> -CNOH	0.32	5.7	2.7
PhOCH ₃	5.0	8.6	7.7
<i>o</i> -CNOCH ₃	2.0	3.9	2.8
<i>m</i> -CNOCH ₃	1.4	4.6	3.7
<i>p</i> -CNOCH ₃	0.87	5.5	6.4

^a Monitored at fluorescence peak wavelengths. ^b Monitored at 310 nm.

expansion coefficient of the solvent, C_p is the specific heat capacity of the solvent, ρ is mass density of the solvent, and E_λ is the excitation energy per absorbed Einstein (450 kJ mol⁻¹ at 266 nm). The structural volume change per photoconverted mole ΔV_R (ml mol⁻¹) is derived by using the reaction quantum yield Φ_R producing RO⁻ and H₃O⁺ (see Figure 2):

$$\Delta V_R = \Delta V_r / \Phi_R \quad (6)$$

We used sodium dichromate (Na₂Cr₂O₇) as a photocalorimetric reference in aqueous solution at 266 nm excitation. The thermal conversion efficiency α of Na₂Cr₂O₇ can be assumed to be unity.^{36c} The PA signal amplitude of the photocalorimetric reference at temperature T is represented by

$$H_T^R = k\Delta V_{th} = k\left(\frac{\beta}{C_p\rho}\right)E_\lambda \quad (7)$$

At the temperature $T_{\beta=0} = 3.9$ °C for which the thermal expansion coefficient of water is zero, the PA signal of the sample solution $H_{T_{\beta=0}}^S$ is given by the structural volume change alone:

$$H_{T_{\beta=0}}^S = k\Delta V_r \quad (8)$$

Therefore, ΔV_r can be related to the ratio of $H_{T_{\beta=0}}^S$ to H_T^R as

$$\frac{H_{T_{\beta=0}}^S}{H_T^R} = \frac{\Delta V_r}{E_\lambda} \left(\frac{C_p\rho}{\beta} \right) \quad (9)$$

The measurement of the structural volume change based on eq 9 is called two-temperature method.³⁶ Thus, ΔV_r can be estimated by taking the PA signal ratio of the sample at $T_{\beta=0}$ to the reference at T .

If an excited cyanophenol molecule dissociates into a solvent-stabilized ion pair in water, substantial volume contraction arising from electrostriction of water around the ions is expected to occur. Figure 6 shows the PA signals of PhOH and CNOHs in H₂O at 3.9 °C, along with the signal of Na₂Cr₂O₇. They were obtained for the solutions with almost the same absorbance (~0.2) at the excitation wavelength. The reference compound Na₂Cr₂O₇ is known to deactivate very rapidly from the excited state with a quantum yield of nearly unity; that is, it releases all the excitation photon energy as heat. The almost no signal

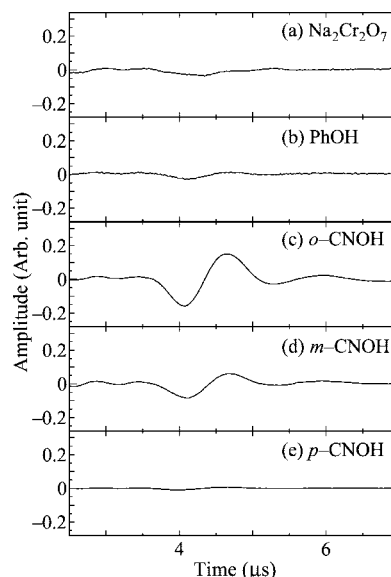


Figure 6. PA signals for (a) the calorimetric reference Na₂Cr₂O₇, (b) PhOH, (c) *o*-CNOH, (d) *m*-CNOH, and (e) *p*-CNOH in H₂O (pH 4.0) at 3.9 °C.

of Na₂Cr₂O₇ in Figure 6 clearly shows that the contribution of thermal expansion to PA signal is negligible under this condition and the PA signal originates solely from structural volume changes. For *o*- and *m*-CNOH, clear PA signals, which correspond to volume contractions, are seen. On the basis of the deconvolution analyses of the PA waveforms, the volume changes per absorbed Einstein (ΔV_r) for *o*- and *m*-CNOH were obtained to be -5.0 and -2.4 mL Einstein⁻¹, respectively (see Supporting Information). The volume contraction per mole (ΔV_R) can be calculated from eq 6 by using the formation quantum yield $\Phi(\text{RO}^-)$ of free RO⁻. As can be seen from Figure 2, $\Phi(\text{RO}^-)$ would be less than unity even if the quantum yield of proton dissociation ($\Phi_{\text{dis}} = k_{\text{dis}}/(k_f + k_{\text{nr}} + k_{\text{dis}})$) is unity, because the rapid decay of (RO⁻...H₃O⁺) is expected to lead to the geminate recombination in the ground-state ion pair. The geminate recombination yield is denoted by $1-\eta$ in Figure 2.

We also measured the volume contraction following proton dissociation of excited 1-naphthol in water based on the PA measurements and obtained $\Delta V_R = -16.4$ mL mol⁻¹ (see Supporting Information). This is in good agreement with the value ($\Delta V_R = -15.8$ mL mol⁻¹)³⁷ obtained by similar PA measurements and that ($\Delta V_R = -17.2$ mL mol⁻¹)³⁸ measured by dilatometry. By assuming that the quantum yield for the formation of free RO⁻ ($\Phi(\text{RO}^-)$) from *o*-CNOH is unity, the volume contraction (ΔV_R) accompanying the ESPT reaction of *o*-CNOH becomes -5.0 mL mol⁻¹, which is much smaller than the ΔV_R values (-12.9 and -13.0 mL mol⁻¹, respectively)³⁹ estimated from the partial molar volumes for the ground-state proton dissociation reactions of *m*-CNOH and *p*-CNOH (the partial molar volumes related to ΔV_R of *o*-CNOH were not available in the literature). An explanation for this disagreement can be proposed as follows. As shown in Figure 2, if the geminate recombination in the ground-state ion pair (RO⁻...H₃O⁺) occurs after rapid deactivation of the excited ion pair (RO^{-*}...H₃O⁺), $\Phi(\text{RO}^-)$ becomes less than unity, and the apparent volume contraction might become significantly smaller than the value calculated by partial molar volumes. As is pointed out by Agmon,³⁵ if the acidity of a ground-state molecule is much smaller than that in the S₁ state, as in the case of naphthols and phenols, a considerable fraction of the ion pairs produced by an ESPT reaction may recombine in the

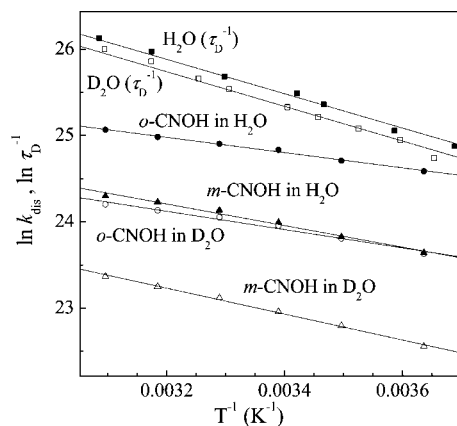


Figure 7. Arrhenius plot of the proton dissociation rate constant of *o*-CNOH in H₂O (pH 2.9) and D₂O (pD 2.7), *m*-CNOH in H₂O and D₂O, and the reciprocal of the Debye dielectric relaxation time τ_D of H₂O and D₂O.

TABLE 3: Proton Dissociation Rate Constant (k_{dis}), Activation Energy (E_a), Frequency Factor (A), and Isotope Effect ($k_{\text{dis}}^{\text{H}}/k_{\text{dis}}^{\text{D}}$)^a for ESPT Reactions of Cyanophenols in H₂O (pH 2.9) and D₂O (pD 2.7)

solvent	k_{dis} (10^{10} s^{-1})	E_a (kJ mol ⁻¹)	A (10^{12} s^{-1})	$k_{\text{dis}}^{\text{H}}/k_{\text{dis}}^{\text{D}}$
<i>o</i> -CNOH				
H ₂ O	6.6	7.3	1.2	2.4
D ₂ O	2.8	8.8	0.9	
<i>m</i> -CNOH				
H ₂ O	2.6	10	1.6	2.8
D ₂ O	0.93	13	1.6	

^a At 298 K.

ground state. Because the recombination probability is larger for pairs which have not separated too much while in the excited state, the ground-state recombination probability is expected to be larger for an excited molecule with a shorter S_1 lifetime. The extremely short lifetimes of *o*-CNO^{-*} and *m*-CNO^{-*} are consistent with the explanation of the observed volume contraction on the basis of ground-state geminate recombination. If one assumes that for *o*-CNOH the quantum yield of proton dissociation (Φ_{dis}) is unity and the magnitude of ΔV_R is the same as those (13 mL mol⁻¹) of *m*-CNOH and *p*-CNOH, the η value in Figure 2 can be estimated to be 0.38.

The volume contractions observed for *o*- and *m*-CNOH demonstrate the occurrence of ESPT process which results in ion-pair formation. From the fluorescence decay time (37 ps) of *m*-CNOH and that (1.4 ns) of *m*-CNOCH₃ in H₂O, the proton dissociation rate constant of *m*-CNOH was estimated to be $2.6 \times 10^{10} \text{ s}^{-1}$, which is somewhat smaller than that of *o*-CNOH.

Proton Dissociation of Cyanophenols in the Excited State.

We measured the proton dissociation rate constant of *o*- and *m*-CNOH in H₂O and D₂O under different temperatures. The Arrhenius plot of the obtained k_{dis} values is depicted in Figure 7. In the temperature range between 275 and 323 K, a linear relationship between $\ln k_{\text{dis}}$ and $1/T$ is seen for both the H₂O and D₂O solutions. From the straight lines in Figure 7, the activation energies for the proton dissociation reactions of *o*-CNOH in H₂O and D₂O were obtained to be 7.3 and 8.8 kJ mol⁻¹, respectively (see Table 3). For *m*-CNOH, somewhat larger E_a values, 10 and 13 kJ mol⁻¹, were found for the H₂O and D₂O solutions, respectively. In both compounds, the D₂O solution gives a slightly larger E_a value compared to that of the H₂O solution (see Table 3). In order to compare the proton dissociation rate with the solvent relaxation rate, the inverse of

the Debye dielectric relaxation time (τ_D) of H₂O and D₂O^{40–42} is plotted as a function of $1/T$ in Figure 7. It can be seen that the proton dissociation rate of *o*- and *m*-CNOH in H₂O and D₂O is slower than the solvent relaxation rate evaluated from the Debye dielectric relaxation time, which is related to the collective structural rearrangement of the hydrogen-bonded liquid enabling the individual molecules to reorient.⁴² In addition, much larger deuterium isotope effects are seen in the proton transfer rates of *o*- and *m*-CNOH as compared with those in the solvent relaxation rate. This behavior is in accord with an activation-controlled reaction along the proton coordinate.

Robinson et al.^{12,14} and Huppert et al.⁴³ have reported that weak photoacids, such as 2-naphthol, behave in an Arrhenius fashion, giving a linear dependence of $\ln k_{\text{dis}}$ on $1/T$ between the freezing and boiling temperatures of water. Its activation energy is $E_a \approx 11 \text{ kJ mol}^{-1}$. Only in supercritical or supercooled water, some downward deviation from the Arrhenius behavior is seen. In contrast, stronger photoacids, such as 8-hydroxypyrene-1,3,6-trisulfonate¹⁵ or 2-hydroxynaphthalene-6,8-disulfonate in water, exhibit a strongly curved Arrhenius plot; that is the reaction activation energy is temperature-dependent. These compounds and also 1-naphthol¹² have $E_a \approx 0$ at high temperatures, suggesting a negligible barrier along the proton coordinate. Huppert et al.¹⁵ have suggested that at low temperatures, solvent motion with characteristic time close to τ_D controls the proton transfer rate, whereas at the high-temperature limit, the solvent-relaxation time is faster than the passage of the proton over the barrier, and the overall rate constant is determined by the proton motion. The kinetic behavior of *o*-CNOH in H₂O and D₂O seems to be somewhat different from that of the above compounds. The prototropic properties of *o*-CNOH, as exemplified by the $\text{p}K_a^*$ value (-0.5) and the fast proton dissociation rate, are in conformity with a relatively strong photoacid. Nevertheless, it has a nearly constant activation energy (7.3 kJ mol⁻¹ in H₂O) even at higher temperatures.

Our results showed that PhOH has moderate acidity ($\text{p}K_a^* > 0$), even in the S_1 state, and the k_{dis} value of PhOH in water can be evaluated to be less than $1.3 \times 10^8 \text{ s}^{-1}$ from eq 3 and Table 2. This is in contrast with 1- and 2-naphthols which undergo ESPT in water. The proton dissociation rate in the excited state is enhanced considerably by introducing an electron-withdrawing group at proper position(s). As for PhOH, it was found that the ortho-position is the most effective site to enhance the excited-state acidity, and the k_{dis} value ($6.6 \times 10^{10} \text{ s}^{-1}$) was increased by more than one-order of magnitude by introducing a cyano group at the *o*-position. The para-position is, on the other hand, found to be less effective to enhance the excited-state acidity; the k_{dis} value is estimated to be less than $2.0 \times 10^9 \text{ s}^{-1}$. Recently, Hynes et al.⁴⁴ have made theoretical investigations on excited-state acidities of PhOH and CNOHs. They have proposed that the $n-\pi^*$ CT on the anion side of the reaction, and not the one on the acid side, is the fundamental origin of the enhanced excited-state acidity. They have also proposed a theoretical equation to calculate the rate constant of proton transfer in hydrogen-bonded acid–base complexes such as phenol–trimethylamine in methyl chloride solvent.⁴⁵ The extension of π -electronic systems can also modify the excited-state acidity of PhOH. Recently, Lewis et al.⁴⁶ have reported that the 4-cyanohydroxystilbenes undergo ESPT with rate constants of $5 \times 10^{11} \text{ s}^{-1}$. These rate constants are comparable to the fastest among the ESPT rate reported so far^{34,47,48} and approach the theoretical limit for water-mediated proton transfer.

In recent studies, the neutral form of the chromophore (*p*-hydroxybenzylidene-imidazolidinone) in wtGFP is reported

to undergo ESPT upon photoexcitation and to result in characteristic green (508 nm) emission.^{23–26} The photophysics of *p*-hydroxybenzylidene dimethylimidazolinone (*p*-HBDI), a model chromophore of GFP, in solution has also been investigated through ultrafast fluorescence spectroscopy.^{49,50} The ESPT to solvent in the model compound *p*-HBDI has not been observed because of ultrafast internal conversion through specific structural displacement. The protein–chromophore interaction in wtGFP leads to the suppression of the radiationless decay and should also be responsible for the occurrence of ESPT in GFP. Despite the fact that the chromophore of wtGFP can be regarded as a *p*-substituted phenol, wtGFP is reported to undergo ESPT. This seems to be in conflict with our observation that *p*-substitution is not effective to enhance photoacidity of phenol by introducing an electron-withdrawing CN group. However, the results of Lewis et al.⁴⁶ on the 4-cyanohydroxystilbenes seem to suggest that the extension of π -electronic conjugation through the *p*-position can also enhance the photoacidity of phenol.

Conclusion

The picosecond time-resolved fluorescence measurements of PhOH and CNOHs revealed that *o*- and *m*-CNOH in H₂O undergo ESPT with rate constants of 6.6×10^{10} and $2.6 \times 10^{10} \text{ s}^{-1}$, respectively, at 298 K. These rates are slower than the solvent relaxation rate evaluated from the Debye dielectric relaxation time (τ_D) of water at 298 K, which suggests that the overall rate constant is determined by the proton motion along the reaction coordinate. The PA spectroscopy was used as a complementary method to examine the ESPT of PhOH and CNOHs. The analysis of the obtained PA signals showed that photoexcitation of *o*-CNOH and *m*-CNOH in H₂O results in volume changes (ΔV_r) of -5.0 and $-2.4 \text{ mL Einstein}^{-1}$, respectively. The observation of volume contractions is consistent with the occurrence of ESPT which gives a solvent-separated ion pair (hydrated proton and phenolate anion). In contrast to *o*- and *m*-CNOH, the excitation of PhOH and *p*-CNOH in H₂O showed negligibly small volume changes. The results of PA measurements and the fluorescence properties of PhOH and *p*-CNOH indicate that the ESPT rates of these compounds are significantly slower than those of *o*- and *m*-CNOH, and the occurrence of ESPT could not be verified clearly from their fluorescence properties in water. The introduction of a strongly electron-withdrawing group at *o*- or *m*-position in PhOH substantially enhances the proton-transfer ability to solvent in the excited state. If we assume that the quantum yields of the solvent-separated ion pair are unity, the volume changes per mole (ΔV_R) of *o*-CNOH and *m*-CNOH in H₂O were estimated to be -5.0 and -2.4 mL mol^{-1} , respectively, which were much smaller than the ΔV_R values ($-12.9 \text{ mL mol}^{-1}$ and $-13.0 \text{ mL mol}^{-1}$, respectively)³⁹ estimated from partial molar volumes for the ground-state proton dissociation reactions for *m*-CNOH and *p*-CNOH. The disagreement could be attributed to the involvement of ground-state geminate recombination between the ejected proton and cyanophenolate anion after rapid deactivation of the excited ion pair.

Acknowledgment. This work was supported in part by Grant-in-Aid (No 14540465) from the Ministry of Education, Culture, Sports, Science, and Technology of Japan. The authors would like to thank Dr. T. Yoshihara for helpful discussions.

Supporting Information Available: Deconvolution analyses of the PA waveform. This material is available free of charge via the Internet at <http://pubs.acs.org>.

References and Notes

- (1) (a) Förster, T. *Naturwiss.* **1949**, *36*, 186. (b) Förster, T. Z. *Elektrochem.* **1950**, *54*, 42–531.
- (2) (a) Weller, A. Z. *Elektrochem.* **1952**, *56*, 662. (b) Weller, A. Z. *Elektrochem.* **1954**, *58*, 849.
- (3) Martynov, I. Y.; Demyashkevich, A. B.; Uzhinov, B. M.; Kuz'min, M. G. *Russ. Chem. Rev. (Usp. Khim.)* **1977**, *46*, 3.
- (4) Shizuka, H. *Acc. Chem. Res.* **1985**, *18*, 141.
- (5) Kosower, E. M.; Huppert, D. *Annu. Rev. Phys. Chem.* **1986**, *37*, 127.
- (6) Alnaut, L. G.; Formosinho, S. J. J. *Photochem. Photobiol., A* **1993**, *75*, 1.
- (7) Mishra, A. K. Fluorescence of Excited Singlet State Acids in Certain Organized Media: Applications as Molecular Probes In *Understanding and Manipulating Excited State Processes, Molecular and Supramolecular Photochemistry Series*; Ramamurthy, V., Schanze, K. S., Eds.; Marcel Dekker, Inc.: New York, 2001; Vol. 8, Chapter 10.
- (8) Caldin, E. F. *The Mechanisms of Fast Reactions in Solution*; IOS Press: Amsterdam, 2001; Chapter 8.
- (9) Tolbert, L. M.; Solntsev, K. M. *Acc. Chem. Res.* **2002**, *35*, 19.
- (10) Agmon, N. *J. Phys. Chem. A* **2005**, *109*, 13.
- (11) Shizuka, H.; Tobita, S. Proton Transfer Reactions in the Excited States. In *Organic Photochemistry and Photophysics, Molecular and Supramolecular Photochemistry Series*; Ramamurthy, V., Schanze, K. S., Eds.; CRC Press: Boca Raton, 2006; Vol. 14, Chapter 2.
- (12) Lee, J.; Robinson, G. W.; Webb, S. P.; Philips, L. A.; Clark, J. H. *J. Am. Chem. Soc.* **1986**, *108*, 6538.
- (13) Webb, S. P.; Philips, L. A.; Yeh, S. W.; Tolbert, L. M.; Clark, J. H. *J. Phys. Chem.* **1986**, *90*, 5154.
- (14) (a) Robinson, G. W.; Thistlethwaite, P. J.; Lee, J. J. *J. Phys. Chem.* **1986**, *90*, 4224. (b) Robinson, G. W. *J. Phys. Chem.* **1991**, *95*, 10386.
- (15) Poles, W.; Cohen, B.; Huppert, D. *Isr. J. Chem.* **1999**, *39*, 347.
- (16) Solntsev, K. M.; Huppert, D.; Agmon, N.; Tolbert, L. M. *J. Phys. Chem. A* **2000**, *104*, 4658.
- (17) Clower, C.; Solntsev, K. M.; Kowalik, J.; Tolbert, L. M.; Huppert, D. *J. Phys. Chem. A* **2002**, *106*, 3114.
- (18) Genosar, L.; Leiderman, P.; Koifman, N.; Huppert, D. *J. Phys. Chem. A* **2004**, *108*, 1779.
- (19) Wehry, E. L.; Rogers, L. B. *J. Am. Chem. Soc.* **1965**, *87*, 4234.
- (20) Schulman, S. G.; Vincent, W. R.; Underberg, W. J. M. *J. Phys. Chem.* **1981**, *85*, 4068.
- (21) Chalfie, M.; Kain, S. *Green Fluorescent Protein: Properties, Applications, and Protocols*; Wiley-Liss: New York, 1998.
- (22) Tsien, R. Y. *Annu. Rev. Biochem.* **1998**, *67*, 509.
- (23) Chatteraj, M.; King, B. A.; Bublitz, G. U.; Boxer, S. G. *Proc. Natl. Acad. Sci. U.S.A.* **1996**, *93*, 8362.
- (24) Stoner-Ma, D.; Jaye, A. A.; Ronayne, K. L.; Nappa, J.; Meech, S. R.; Tonge, P. J. *J. Am. Chem. Soc.* **2008**, *130*, 1227.
- (25) Leiderman, P.; Gepshtein, R.; Tsimberov, I.; Huppert, D. *J. Phys. Chem. B* **2008**, *112*, 1232.
- (26) Gepshtein, R.; Leiderman, P.; Huppert, D. *J. Phys. Chem. B* **2008**, *112*, 7203.
- (27) Eaton, D. F. *Pure Appl. Chem.* **1988**, *60*, 1107.
- (28) Perichet, R. G.; Chaperon, R.; Pouyet, B. *J. Photochem.* **1980**, *13*, 67.
- (29) Oshima, J.; Shiobara, S.; Naoumi, H.; Kaneko, S.; Yoshihara, T.; Mishra, A. K.; Tobita, S. *J. Phys. Chem. A* **2006**, *110*, 4629.
- (30) Tsutsumi, K.; Shizuka, H. *Z. Phys. Chem., Neue Folge* **1980**, *122*, 129.
- (31) Wang, H.; Wang, X.; Li, X.; Zhang, C. *J. Mol. Struct.* **2006**, *770*, 107.
- (32) Grabner, G.; Köhler, G.; Zechner, J.; Getoff, N. *J. Phys. Chem.* **1980**, *84*, 3000.
- (33) Pál, K.; Kállay, M.; Köhler, G.; Zhang, H.; Bitter, I.; Kubinyi, M.; Vidóczy, T.; Grabner, G. *ChemPhysChem* **2007**, *8*, 2627.
- (34) Shiobara, S.; Tajima, S.; Tobita, S. *Chem. Phys. Lett.* **2003**, *380*, 673.
- (35) (a) Agmon, N. *J. Chem. Phys.* **1988**, *89*, 1524. (b) Gopich, I. V.; Solntsev, K. M.; Agmon, N. *J. Chem. Phys.* **1999**, *110*, 2164. (c) Solntsev, K. M.; Huppert, D.; Agmon, N. *Phys. Rev. Lett.* **2001**, *86*, 3427.
- (36) (a) Braslavsky, S. E.; Heibel, G. E. *Chem. Rev.* **1992**, *92*, 1381. (b) Churio, M. S.; Angermund, K. P.; Braslavsky, S. E. *J. Phys. Chem.* **1994**, *98*, 1776. (c) Gensch, T.; Braslavsky, S. E. *J. Phys. Chem. B* **1997**, *101*, 101. (d) Small, J. R.; Libertini, L. J.; Small, E. W. *Biophys. Chem.* **1992**, *42*, 29. (e) Borsarelli, C. D.; Bertolotti, S. G.; Previtali, C. M. *Photochem. Photobiol. Sci.* **2003**, *2*, 791.
- (37) Losi, A.; Viappiani, C. *Chem. Phys. Lett.* **1998**, *289*, 500.

- (38) Hamann, S. D.; Linton, M. *J. Chem. Soc., Faraday Trans. 1* **1974**, 70, 2239.
- (39) Hopkins, H. P., Jr.; Duer, W. C.; Millero, F. J. *J. Solution Chem.* **1976**, 5, 263.
- (40) Rønne, C.; Thrane, L.; Åstrand, P.-O.; Wallqvist, A.; Mikkelsen, K. V.; Keiding, S. R. *J. Chem. Phys.* **1997**, 107, 5319.
- (41) Rønne, C.; Åstrand, P.-O.; Keiding, S. R. *Phys. Rev. Lett.* **1999**, 82, 2888.
- (42) Rønne, C.; Keiding, S. R. *J. Mol. Liq.* **2002**, 101, 199.
- (43) Cohen, B.; Leiderman, P.; Huppert, D. *J. Phys. Chem. A* **2002**, 106, 11115.
- (44) (a) Granucci, G.; Hynes, J. T.; Millie, P.; Tran-Thi, T. H. *J. Am. Chem. Soc.* **2000**, 122, 12243. (b) Hynes, J. T.; Tran-Thi, T. H.; Granucci, G. *J. Photochem. Photobiol., A* **2002**, 154, 3.
- (45) Staib, A.; Borgis, D.; Hynes, J. T. *J. Chem. Phys.* **1995**, 102, 2487.
- (46) (a) Lewis, F. D.; Crompton, E. M. *J. Am. Chem. Soc.* **2003**, 125, 4044. (b) Crompton, E. M.; Lewis, F. D. *Photochem. Photobiol. Sci.* **2004**, 3, 660. (c) Lewis, F. D.; Sinks, L. E.; Weigel, W.; Sajimon, M. C.; Crompton, E. M. *J. Phys. Chem. A* **2005**, 109, 2443.
- (47) Pines, E.; Pines, D.; Barak, T.; Magnes, B. -Z.; Tolbert, L. M.; Haubrich, J. E. *Ber. Bunsen-Ges. Phys. Chem.* **1998**, 102, 511.
- (48) Poizat, O.; Bardez, E.; Buntinx, G.; Alain, V. *J. Phys. Chem. A* **2004**, 108, 1873.
- (49) Mandal, D.; Tahara, T.; Meech, S. R. *J. Phys. Chem. B* **2004**, 108, 1102.
- (50) Gepshtein, R.; Huppert, D.; Agmon, N. *J. Phys. Chem. B* **2006**, 110, 4434.

JP8086489